

A General Algorithm of Flattening Convex Prisms

Li Chenglei, Zhou Jingqi

Mentor: Chai Ming Huang
NUS High School of Mathematics and Science
20 Clementi Avenue 1, 129957 Singapore, Singapore

Abstract

Flattening polyhedra is defined as an origami which flattens 3D polyhedra to 2D flat sheet without tearing. It has wide-ranging applications in real-life from flattening of shopping bags to astronomy, robotics-making to biomedical appliances involving trestles and stents. The most notable advantage of flattening polyhedron is reducing the space taken up by the original 3D structure and this has attracted considerable attention. Demaine and Hayes from “Origami” group in MIT have first shown that all polyhedra have flattened states. However, flattening of polyhedra remains as an open problem in terms of method to find the flattened state of all polyhedra and its continuous folding motion. This report presents an original and novel method for flattening convex prisms. A MATLAB program has been written to implement the algorithm automatically, allowing users to specify a target prism and generate a crease pattern that folds into it.

1 Introduction

Flattening polyhedron has wide-ranging applications in real-life from flattening of shopping bags to astronomy, robotics-making to biomedical appliances involving trestles and stents. The most notable advantage of flattening polyhedron is reducing the space taken up by the original 3D structure and this has attracted considerable attention. By allowing all faces to lie on a single plane, the volume of polyhedron can effectively be reduced to zero. Demaine and Hayes have first shown that all polyhedra have flattened states [1]. However, flattening of polyhedral remains as an open problem in terms of method to find the flattened state of all polyhedral and its continuous folding motion. While Demaine and O'Rourke have proposed the idea of disk-packing from 2D fold-and-cut problem, the disk-packing method is limited to polyhedral which are homeomorphic to a disk or a sphere [2]. In particular, Bern and Hayes have proven that flattened states exist for an orientable piecewise-linear(PL) 2-manifold [3]. However, disk-packing method requires that the polyhedra are extended to 4D in the folding process [2]. The most recent result by J. Itoh, C. Nara and C. Vîlcu [4] has proven that every convex polyhedron possesses infinitely many continuous flat folding processes. In this report, we have proposed a method to flatten all convex prismaticoids. Our proposed method can also be used to flatten convex polyhedral as all convex polyhedra can be sliced into several sections of convex prismaticoids.

Section 2 is on notations and definitions that will be used throughout this paper. Section 3 describes the algorithm for drawing net from projection and height of convex prismaticoid, and also introduces general algorithm for flattening. Section 4 presents the algorithm in detail. Limitation to the algorithm is discussed in section 4 and methods to overcome the limitation have also been derived. Section 5 illustrates the capabilities of our algorithm via several convex polyhedral test examples. Section 6 discusses about applications of flattening polyhedron. Finally, section 7 is on the conclusion and future work.

2 Definitions

Definition 1 (Convex Prismaticoid). (Fig. 1) A convex prismaticoid P is a convex polyhedron in 3D Euclidean Space whose vertices lie among two parallel planes. The planes will be termed the roof plane R and base plane B , and the distance between them will be denoted as h . By convention, we assume that B is the xy -plane, and R is the plane defined by $z = h$. We denote the lateral face as F_n . The F_n lateral face is the n -th lateral face in the counterclockwise direction.

Definition 2 (Projection). A projection is an "aerial view" of the convex prismaticoid, drawn on base plane. Formally, it is the image of the points of the prismaticoid under the map $(x, y, z) \mapsto (x, y, 0)$.

We denote r_n as -- the edge of lateral face F_n which lies in R . If that edge is merely a

point, we treat it as segment r_n with length 0. Then F_n is a triangular lateral face whose apex lies in R .

We denote b_n as -- the edge of lateral face F_n which lies in B . If that edge is merely a point, we treat it as segment b_n with length 0. Then F_n is a triangular lateral face whose apex lies in B .

For edges that neither lie in R nor B , and is shared by lateral faces F_n and F_{n+1} , is denoted by s_n .

The height of lateral face F_n is denoted by t_n . The projection of t_n , which is also the projected distance between r_n and b_n , is denoted by l_n .

When a vertex on R is surrounded by $(m+1)$ faces: $R, F_n, F_{n+1} \dots F_{n+m-1}$, we denote this vertex as $p_{n,n+m-1}$. Similarly, when a vertex on B is surrounded by $(m+1)$ faces: $B, F_n, F_{n+1} \dots F_{n+m-1}$, we denote this vertex as $q_{n,n+m-1}$.

Lateral face F_n is either triangular or quadrilateral. On any quadrilateral lateral face F_n , we denote the angles in clockwise direction as $\alpha_{n1}, \alpha_{n2}, \alpha_{n3}$ and α_{n4} , with angles α_{n1} and α_{n2} adjacent to R ; angles α_{n3} and α_{n4} , adjacent to B . α_{n1} and α_{n4} are supplementary angles; α_{n2} and α_{n3} are supplementary angles.

Triangular lateral face F_n , is merely a quadrilateral lateral face F_n whose $r_n = 0$ or $b_n = 0$. Again, we denote the angles in clockwise direction as $\alpha_{n1}, \alpha_{n2}, \alpha_{n3}$ and α_{n4} .

For F_n whose $r_n = 0$, we denote its apex angle adjacent to R as α_{n0} . $\alpha_{n0} = \alpha_{n1} + \alpha_{n2} - 180^\circ$. For F_n whose $b_n = 0$, we denote its apex angle adjacent to B as α_{n5} . $\alpha_{n5} = \alpha_{n3} + \alpha_{n4} - 180^\circ$.

For vertex $p_{n,n+m-1}$, its corresponding angle on R is denoted by $\beta_{n,n+k-1}$. Similarly, for vertex $q_{n,n+m-1}$, its corresponding angle on B is denoted by $\gamma_{n,n+k-1}$.

The dihedral angle between planes of F_n and F_{n+1} on R is β_n . The dihedral angle between planes of F_n and F_{n+1} on B is γ_n . R and B are parallel, so $\beta_n = \gamma_n$.

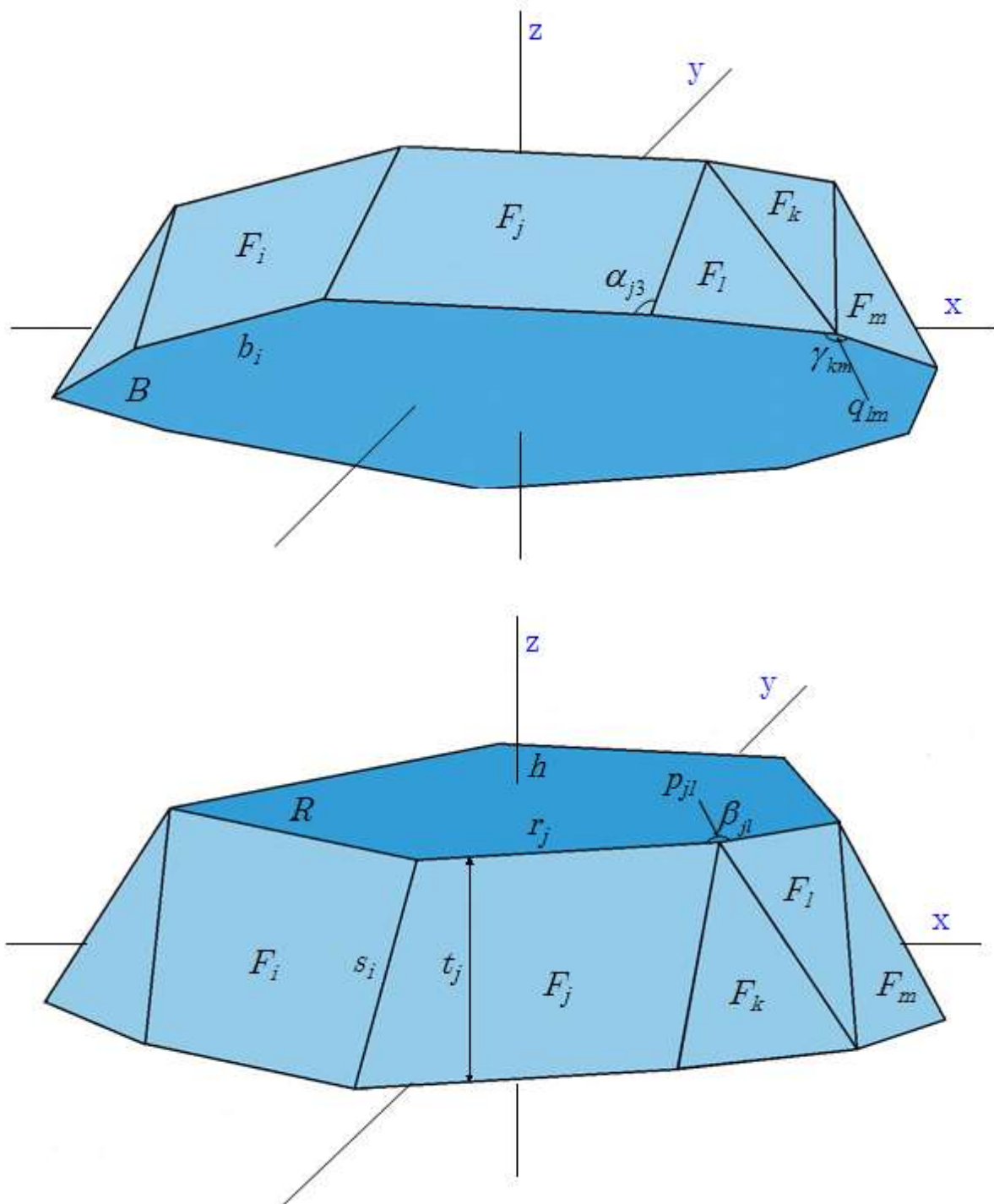


Fig 1: Notations on convex prismaoid

Definition 3 (Net). The net N of a convex prismaoid is obtained by removing the face on the roof plane, and unfolding each lateral face F_n onto the base plane, pivoting along an axis parallel to the edge of F_n that lies on the base plane, b_n .

3 Method Overview

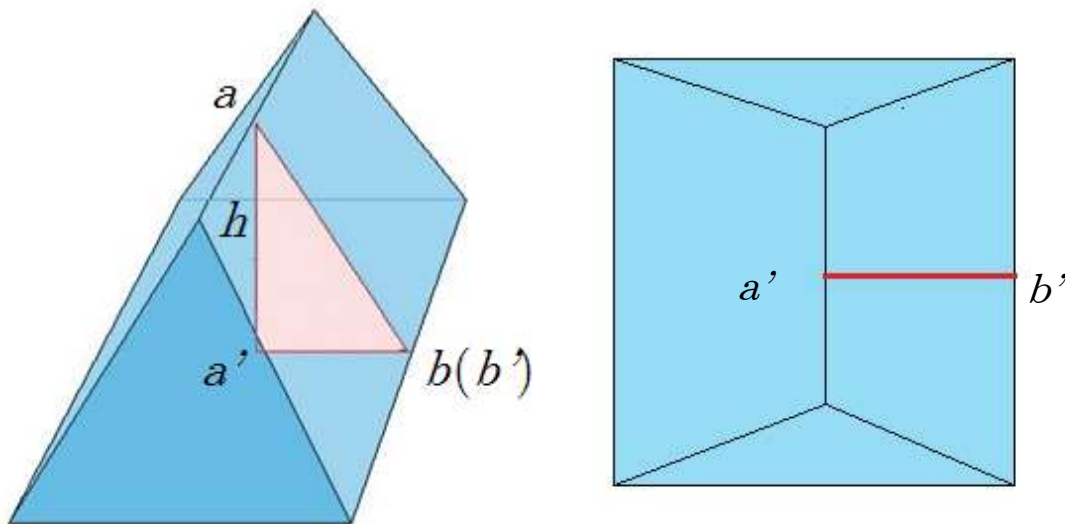
3.1 Obtaining Net from Projection and Height

Lemma 1 Given the projection and height of any convex prismatoid, the length of all edges of lateral faces can be determined. Thus, the net is obtained.

Proof: For any prismatoid, R is parallel to B . Upon projection, any segment that is parallel to either plane retains its length.

For segment that is parallel to neither planes, such as segment \overline{ab} (shown in Fig. 2). Let the segment $\overline{a'b'}$ be the projection of segment \overline{ab} . Since projection and height of any prismatoid are given, the length of \overline{ab} can be obtained by:

$$\overline{ab} = \sqrt{(\overline{a'b'})^2 + h^2}.$$



(a) Visualization of the triangle (b) Projection of segment \overline{ab} for Lemma 1

Fig 2: Visuals for Lemma 1

3.2 Proposed Algorithm

Our main approach is to tuck lateral faces F into spaces between roof plane R and base plane B . The resultant 2D flattened layout will thus be the same as the projection of the 3D polyhedron.

Upon tucking lateral faces F into spaces between R and B , a "five valley line" crease pattern will emerge on each F . One "middle valley line" is parallel to R and B , another four valley lines extend from four vertices of lateral face F . (Fig. 3)

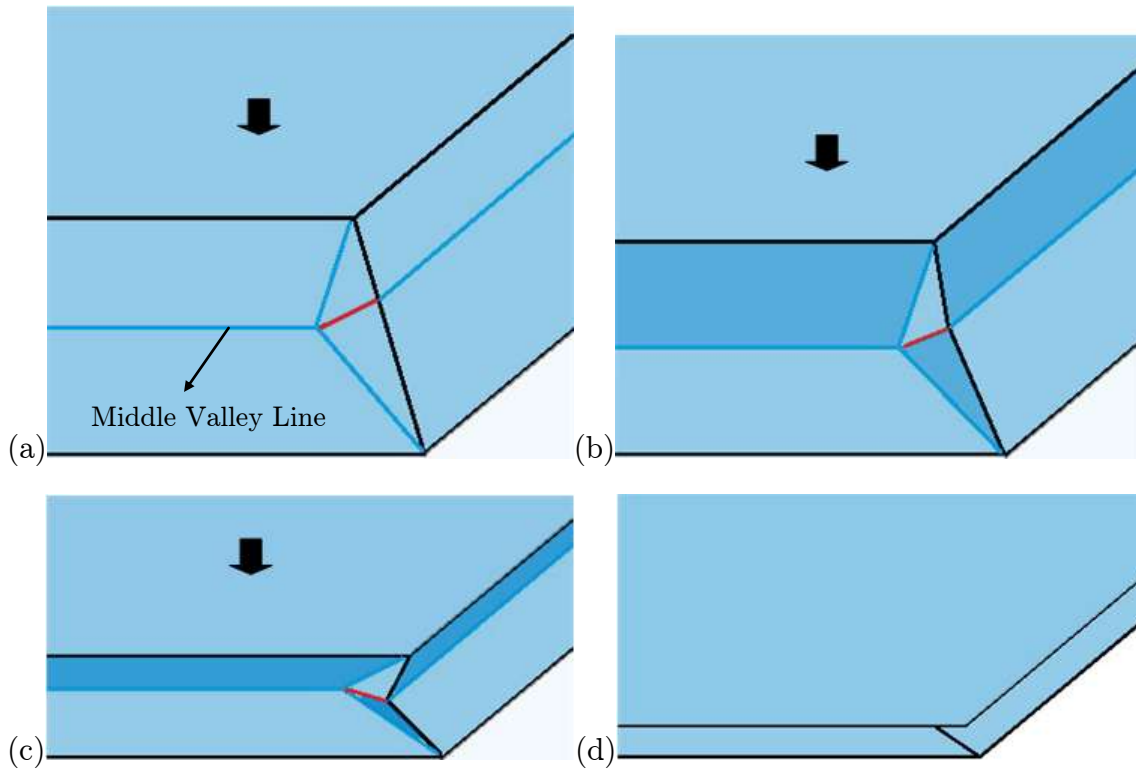


Fig 3: Side view of the emergence of "Middle Valley Line"

Algorithm for drawing crease pattern on any pramatoid (when projection and height of a pramatoid are given)

1. Draw net by applying Lemma 1.
2. Check conditions by applying Proposition 7 and Theorem 8, slice the convex pramatoid horizontally if limitation exists.
3. Draw "middle valley line" for each lateral face by applying Proposition 2.
4. Draw another four valley lines on each lateral face by applying Theorem 4 and Corollary 5. Thus form a "five valley line" crease pattern.
5. According to Proposition 6, erase the unnecessary crease patterns.
6. Add mountain lines accordingly.

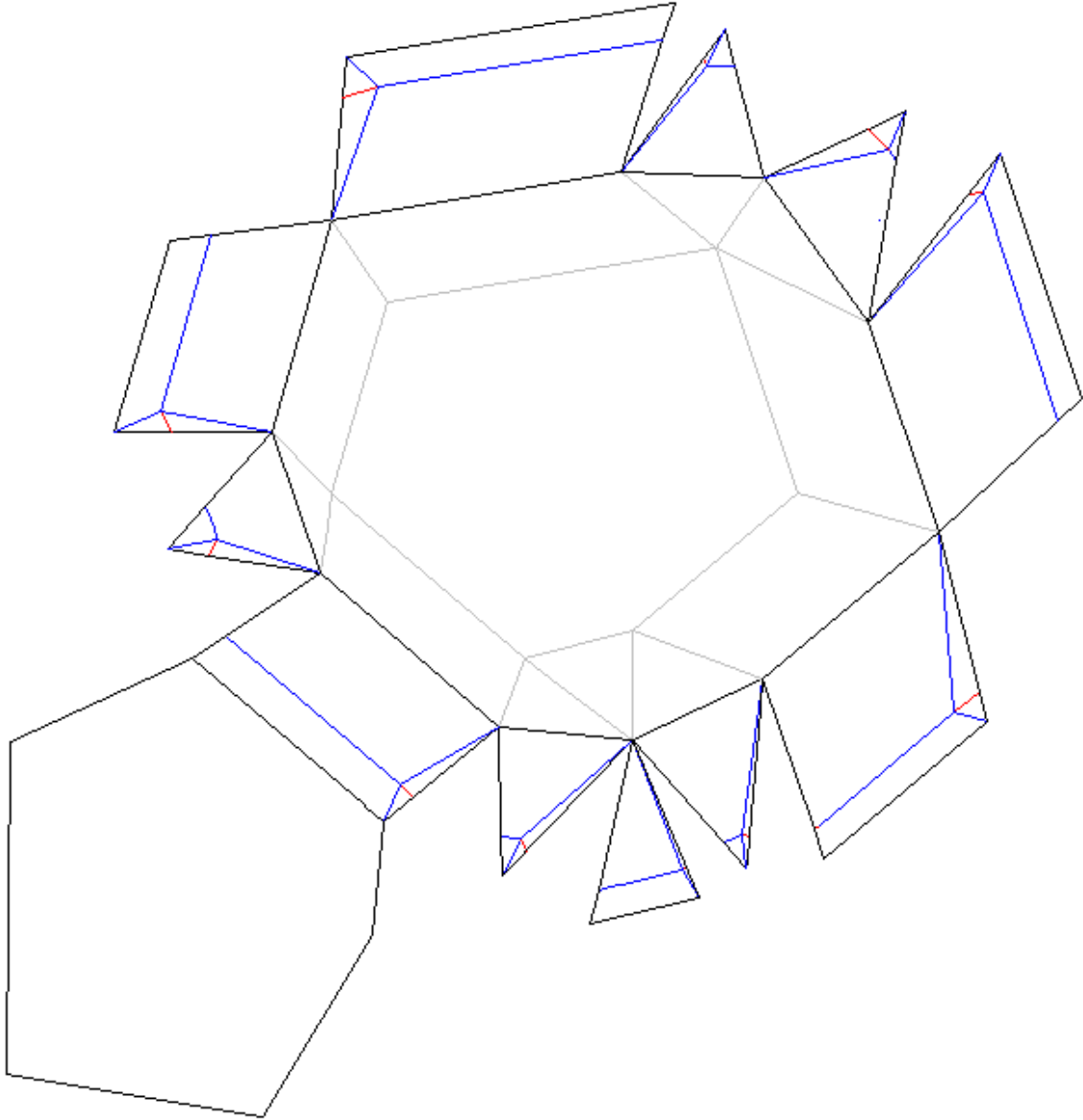


Fig 4: Resultant crease pattern
(red lines, blue lines, grey lines represent mountain, valley and projection respectively)

4 Main result

4.1 Algorithm for drawing of middle valley lines

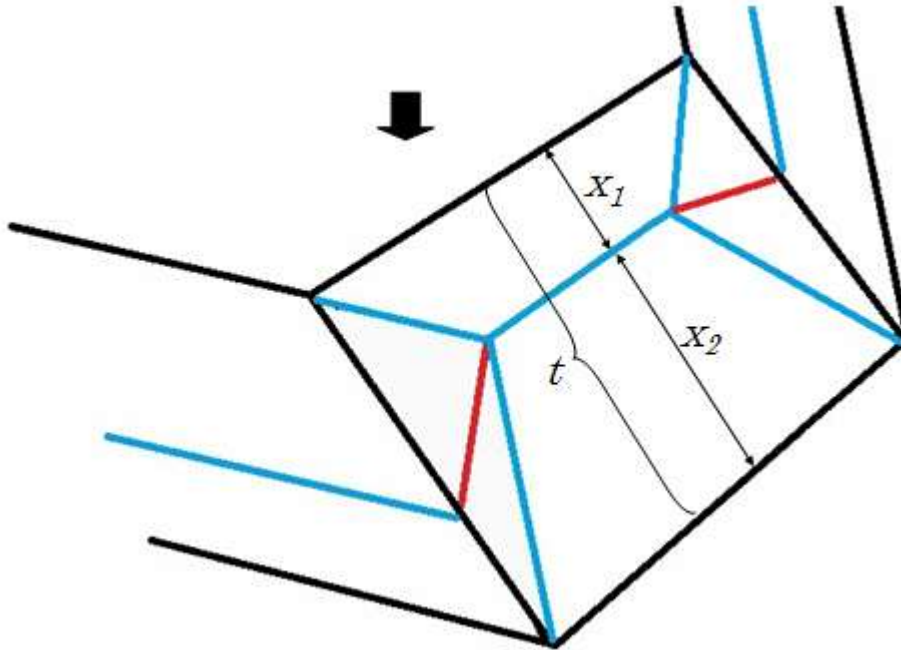
Proposition 2 Let x_r denotes the distance from roof segment r to the "middle valley line"; x_b denotes the distance from base segment b to the "middle valley line".

$$x_1 = \frac{t-l}{2} \quad \text{and} \quad x_2 = \frac{t+l}{2}.$$

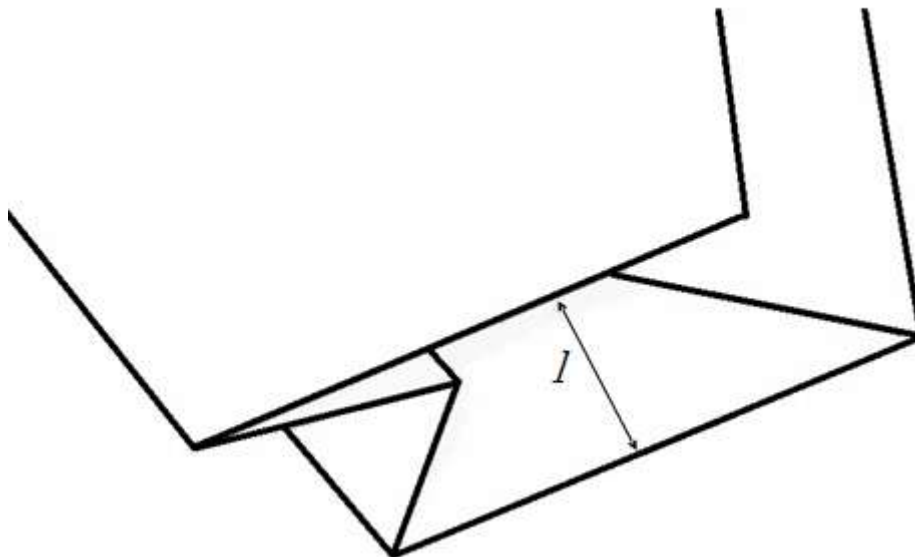
Proof: Since the layout of resultant pattern upon flattening is the same as the layout of projection of the pramatoid, the "middle valley line" on each lateral face F is parallel to R and B .

The "middle valley line" divides F into two portions which overlap in the flattened state (shown in Fig. 5b). The heights of these two portions are x_1 and x_2 respectively.

From $x_1 + x_2 = t$ and $x_2 - x_1 = l$, we obtain $x_1 = \frac{t-l}{2}$ and $x_2 = \frac{t+l}{2}$.



(a) lateral face F before flattening



(b) flattened state of F

Fig 5: Overlap of two portions (with height x_1 and x_2) of lateral face F upon folding

We denote the dihedral angle between each lateral face and base plane as δ (Fig. 6). Then, $l = t \cdot \cos \delta$.

$$\text{And, } x_1 = \frac{t(1 - \cos \delta)}{2},$$

$$x_2 = \frac{t(1 + \cos \delta)}{2}.$$

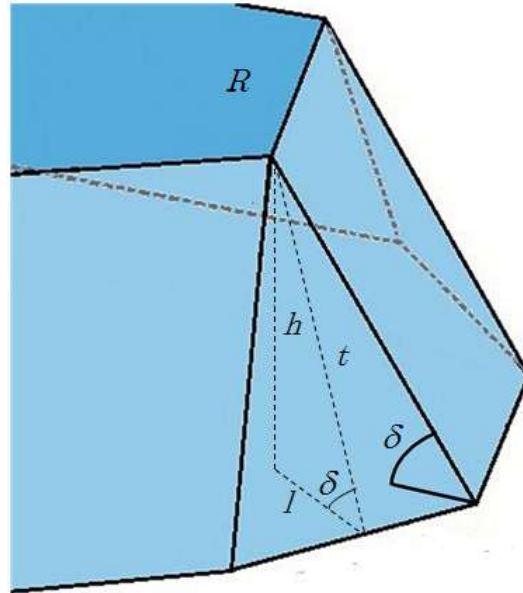
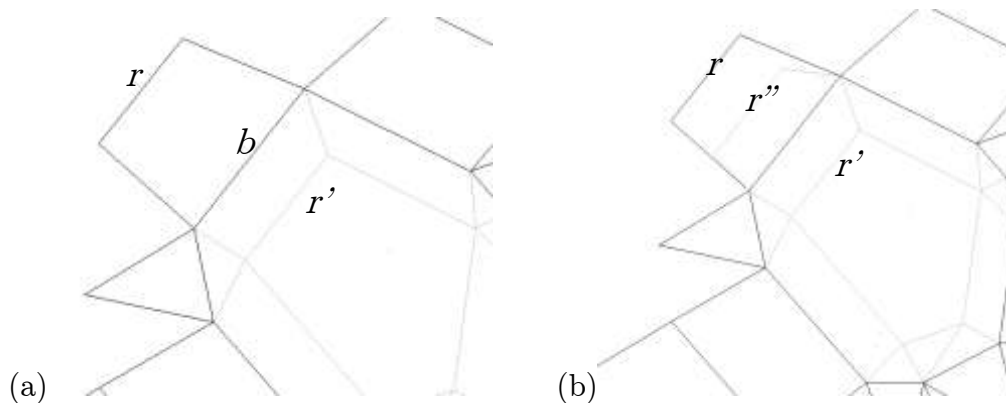


Fig 6: Notation of dihedral angle δ

Algorithm Step 3 (Drawing of "middle valley line" if no limitation exists) (Fig. 7)

- Start with the net. Grey lines represent projection of prismatic and are for construction. b is a base edge, and r was a roof edge before the lateral face was "unfolded" into the net. That roof edge was projected onto r' .
- Reflect r' about the axis (parallel to r') along b onto a new segment r'' .
- Construct the line (shown in blue) of points equidistant from r and r'' , make sure that it is parallel to r and b .
- The grey lines constructed in step (b) can now be omitted.



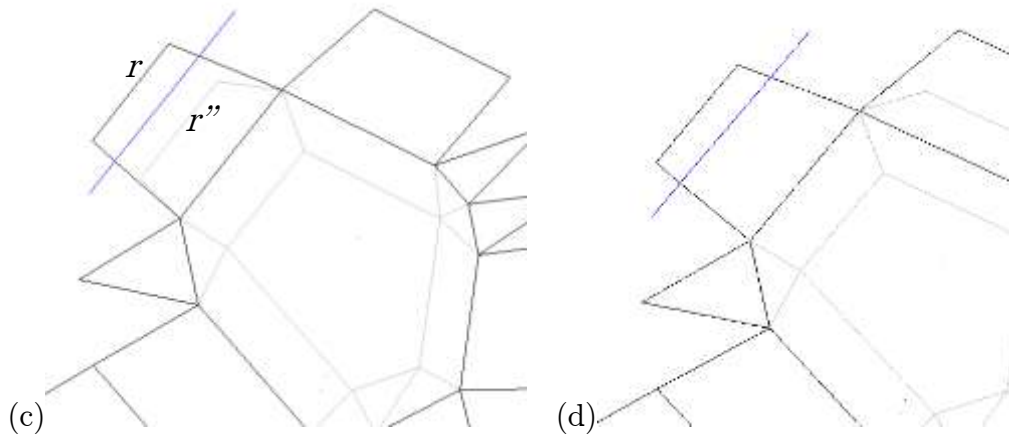


Fig 7: Algorithm Step 3 (Drawing of "middle valley line")

4.2 Algorithm for drawing another four valley lines

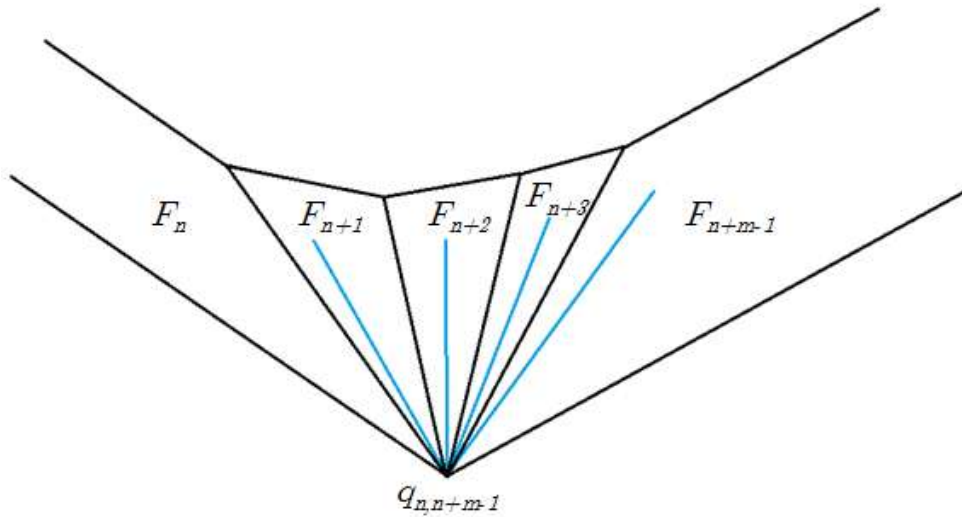
Lemma 3 (Fig. 8a) For a vertex $q_{n,n+m-1}$ on base plane surrounded by $(m+1)$ faces (1 B and m lateral faces), upon flattening, there are $(m+1)$ mountain folds and $(m-1)$ valley folds extending from $q_{n,n+m-1}$. In addition, the $(m-1)$ valley folds are drawn on any $(m-1)$ lateral faces of the m lateral faces.

This holds for any vertex $p_{n,n+m-1}$ on roof plane as well.

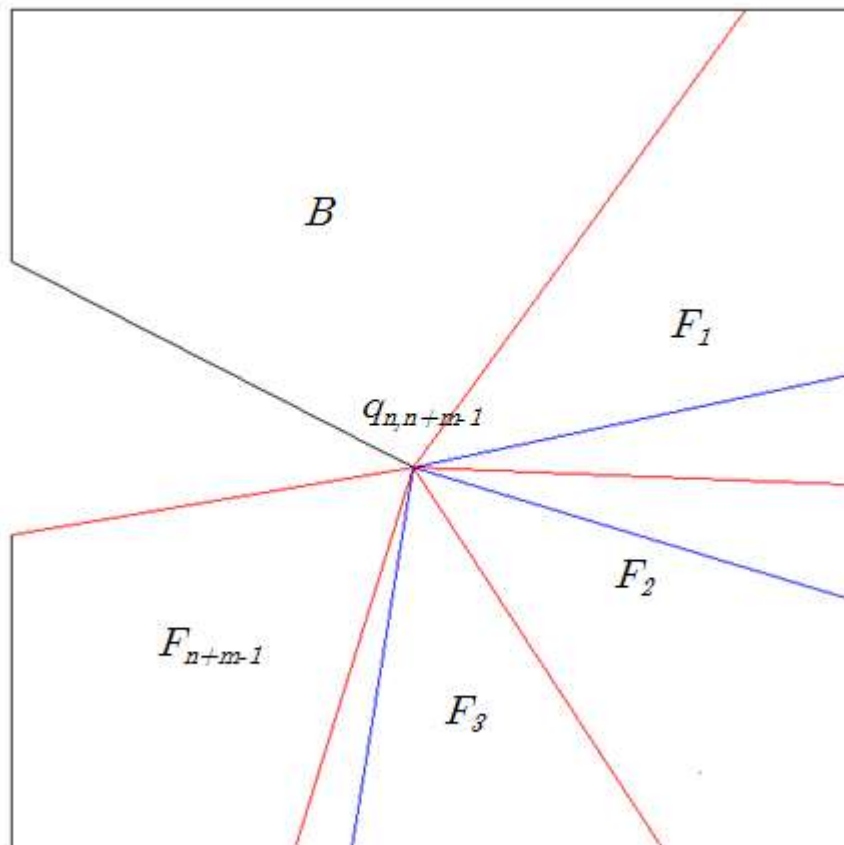
Proof: A vertex $q_{n,n+m-1}$ on base plane is surrounded by $(m+1)$ faces (1 B and m lateral faces). The m lateral faces are: $F_n, F_{n+1}, F_{n+2}, \dots, F_{n+m-1}$. The $(m+1)$ mountain folds are: b_n, b_{n+m-1} and $s_n, s_{n+1}, \dots, s_{n+m-2}$. This implies that $F_{n+1}, F_{n+2}, \dots, F_{n+m-2}$ are triangular lateral faces whose apex lie on B .

Similarly, a vertex $p_{n,n+m-1}$ on roof plane is surrounded by $(m+1)$ faces (1 R and m lateral faces). The m lateral faces are: $F_n, F_{n+1}, F_{n+2}, \dots, F_{n+m-1}$. The $(m+1)$ mountain folds are: r_n, r_{n+m-1} and $s_n, s_{n+1}, \dots, s_{n+m-2}$. This implies that $F_{n+1}, F_{n+2}, \dots, F_{n+m-2}$ are triangular lateral faces whose apex lie on R .

In addition, Maekawa's Theorem states that the number of mountain folds in a flat-folded vertex figure differs from the number of valley folds by exactly two folds (Fig. 8b). Thus, there is one valley fold extending from vertex $q_{n,n+m-1}$ for every two adjacent lateral faces: F_n and F_{n+1} ; F_{n+1} and F_{n+2} ; \dots ; F_{n+m-2} and F_{n+m-1} . The total number of valley folds extending from $q_{n,n+m-1}$ is hence $(m-1)$.



(a) Number of valley lines differs mountain lines by two



(b) After unfolding the lateral faces surrounding vertex $q_{n,n+m-1}$

Fig 8: Unfolded lateral faces surrounding vertex $q_{n,n+m-1}$

This holds for vertex $p_{n,n+m-1}$ as well.

For the convenience of visualization, we draw the same valley fold on both adjacent lateral faces. A "five valley line" crease pattern is formed. In the end, we will

keep only two valley folds(one extending from p and the other one from q) for every two adjacent lateral faces, and erase the rest.

The two valley folds(one extending from p and the other one from q) contribute an "excess flap" (Fig. 9) for two adjacent lateral faces, say F_n and F_{n+1} . We denote this "excess flap" as E_n . The vertex angles of E_n are θ_{Rn} and θ_{Bn} , adjacent to R and B respectively.

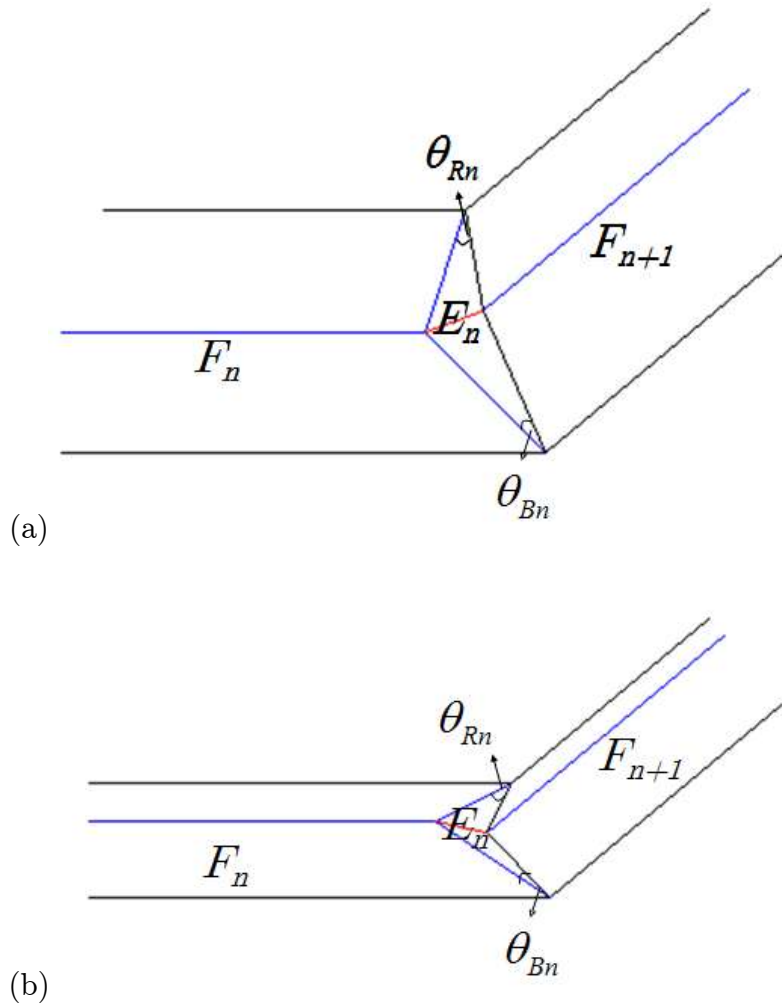


Fig 9: (a) (b) Excess Flap

Theorem 4 (Fig. 10a)At any vertex $q_{n,n+m-1}$, the "excess flaps" are $E_n, E_{n+1}, \dots, E_{n+m-2}$. The corresponding vertex angles are $\theta_{Bn}, \theta_{B(n+1)}, \dots, \theta_{B(n+m-2)}$. And,

$$\sum_{i=n}^{n+m-2} \theta_{Bi} = \frac{\alpha_{n3} + \sum_{i=n+1}^{n+m-2} \alpha_{i5} + \alpha_{(n+m-1)4} - \gamma_{n,n+m-1}}{2}.$$

Similarly, at any vertex $p_{n,n+m-1}$, the "excess flaps" are $E_n, E_{n+1}, \dots, E_{n+m-2}$. The corresponding vertex angles are $\theta_{Rn}, \theta_{R(n+1)}, \dots, \theta_{R(n+m-2)}$. And,

$$\sum_{i=n}^{n+m-2} \theta_{Ri} = \frac{\alpha_{n2} + \sum_{i=n+1}^{n+m-2} \alpha_{i0} + \alpha_{(n+m-1)1} - \beta_{n,n+m-1}}{2}.$$

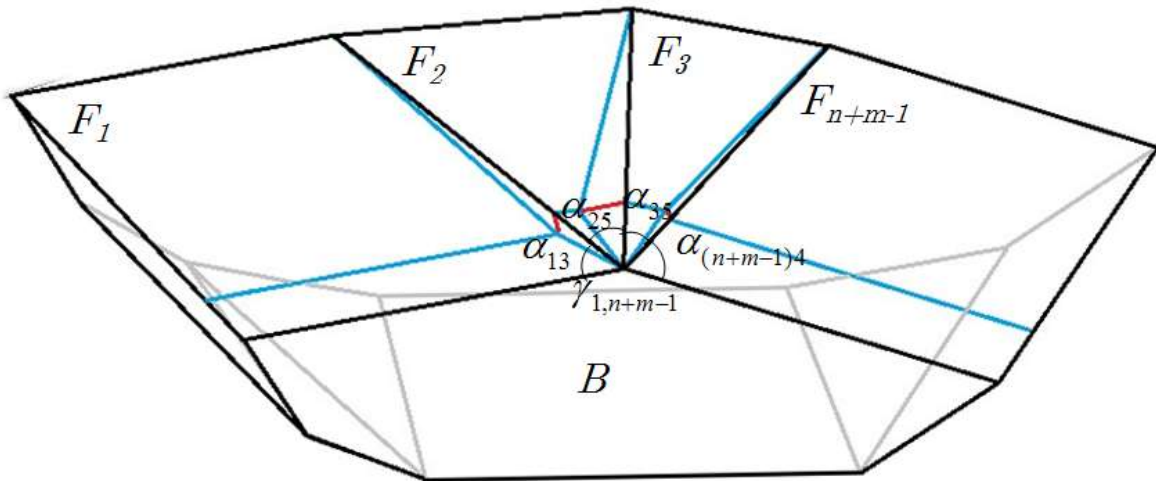
Proof: (Fig. 10b) According to Kawasaki's Theorem, the crease pattern may be folded flat if and only if the alternating sum and difference of the angles adds up to zero.

In our case, the alternating sum and difference of the angles

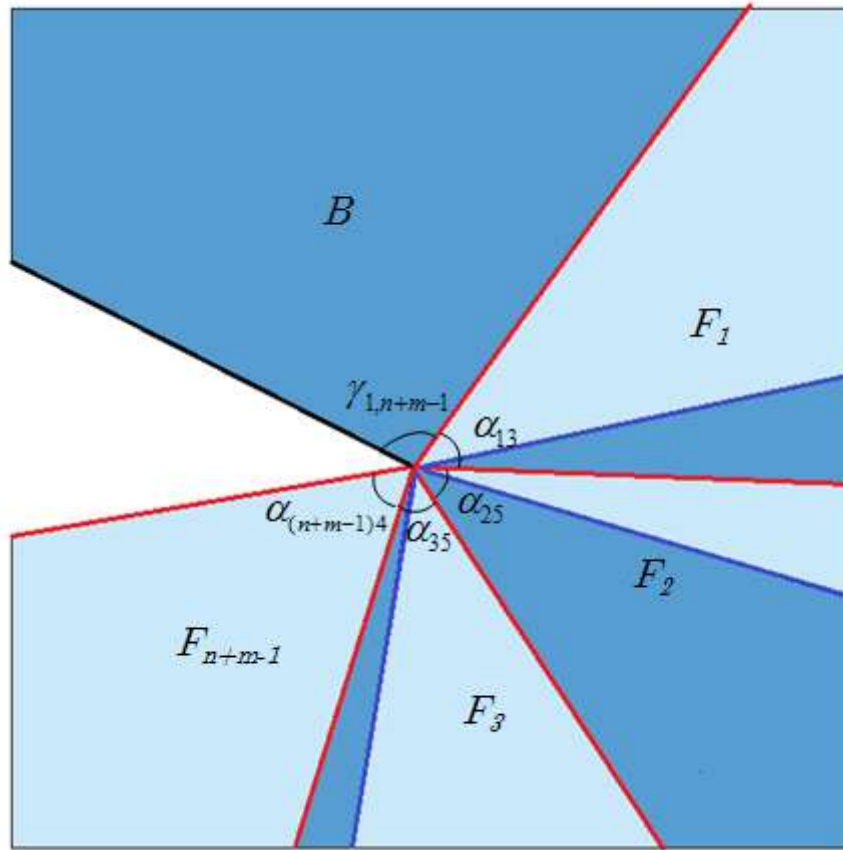
$$= (\alpha_{n3} - \theta_{Bn}) - \theta_{Bn} + (\alpha_{(n+1)5} - \theta_{B(n+1)}) - \dots + \dots - \theta_{B(n+m-2)} + \alpha_{(n+m-1)4} - \gamma_{n,n+m-1}$$

$$= \alpha_{n3} + \sum_{i=n+1}^{n+m-2} \alpha_{i5} + \alpha_{(n+m-1)4} - \gamma_{n,n+m-1} - 2 \sum_{i=n}^{n+m-2} \theta_{Bi}$$

= 0, which agrees with Kawasaki's Theorem.



(a) 3D notation



(b) After unfolding the lateral faces surrounding vertex $q_{n,n+m-1}$

Fig 10: Proof of Proposition 4

Corollary 5 As shown in Fig. 11, when $m+1=3$, vertex $q_{n,n+1}$ is surrounded by three faces, the sole "excess flap" is E_n . Its corresponding angle $\theta_{Bn} = \frac{\alpha_{n3} + \alpha_{(n+1)4} - \gamma_{n,n+1}}{2}$.

In particular (Fig. 12), this is still valid for vertex $q_{n,n+m-1}$ which is surrounded by more than three faces. This time, we deal with the planes of every two consecutive lateral face: $F_n, F_{n+1}; F_{n+1}, F_{n+2}; \dots; F_{n+m-2}, F_{n+m-1}$.

Calculation of the corresponding angle of "excess flap" E_n is again:

$\theta_{Bn} = \frac{\alpha_{n3} + \alpha_{(n+1)4} - \gamma_{n,n+1}}{2}$, where $\gamma_{n,n+1}$ is the dihedral angle between the planes of lateral faces F_n and F_{n+1} .

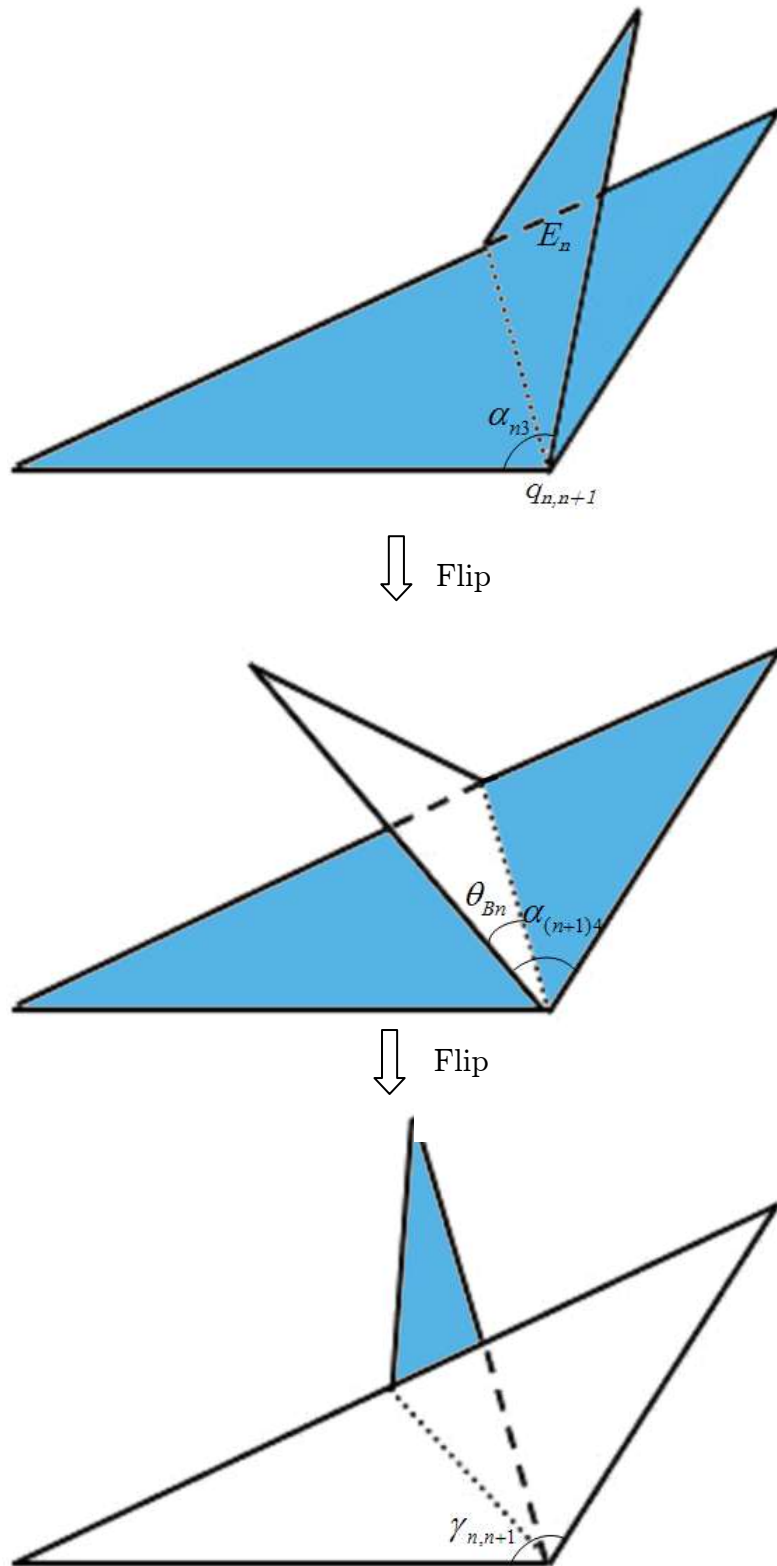


Fig 11: Three lateral faces surrounding a vertex ($m+1=3$)

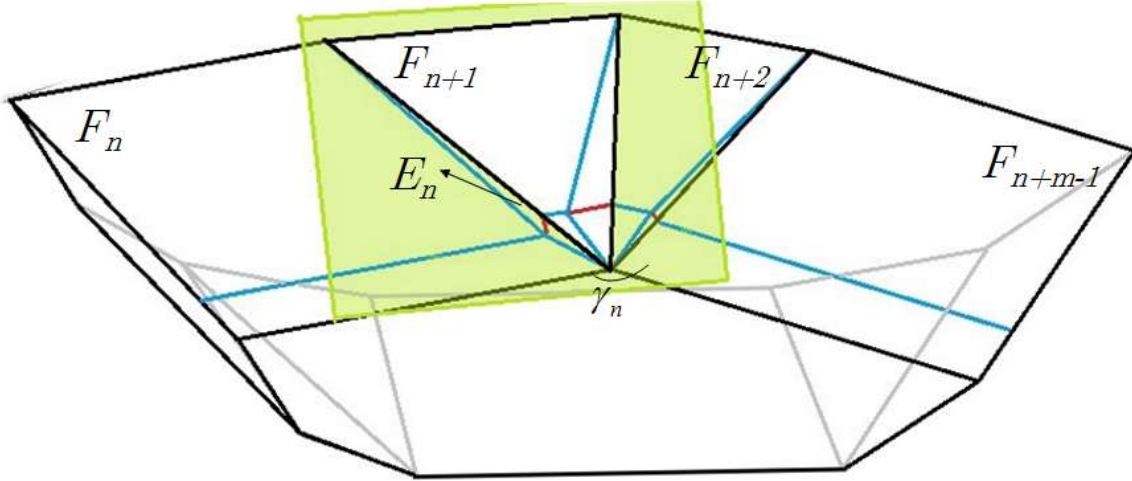


Fig 12: When $q_{n,n+m-1}$ is surrounded by more than three faces

Proof: See projection of prismatoid in Fig. 13, vertex $q_{n,n+m-1}$ is surrounded by 2 quadrilateral lateral faces F_n and F_{n+m-1} , $(m-2)$ triangular lateral faces $F_{n+1}, F_{n+2}, \dots, F_{n+m-2}$. Since R and B are parallel, we translate R to B and form a concave m -gon. The sum of the interior angles in this concave m -gon is:

$$(180^\circ - \gamma_n) + \left((m-3) \cdot 360^\circ - \sum_{i=n+1}^{n+m-3} \gamma_i \right) + (180^\circ - \gamma_{n+m-2}) + \gamma_{n,n+m-1} = (m-2) \cdot 180^\circ$$

$$(m-2) \cdot 360^\circ - \sum_{i=n}^{n+m-2} \gamma_i + \gamma_{n,n+m-1} = (m-2) \cdot 180^\circ$$

$$\sum_{i=n}^{n+m-2} \gamma_i = (m-2) \cdot 180^\circ + \gamma_{n,n+m-1}.$$

From **Definition 2**, the angle of triangular lateral face F_n adjacent to B is calculated by: $\alpha_{n5} = \alpha_{n3} + \alpha_{n4} - 180^\circ$. Thus, $\alpha_{n3} + \alpha_{n4} = \alpha_{n5} + 180^\circ$.

From **Corollary 5**, when dealing with planes of every two consecutive lateral faces:

$$\theta_{Bn(n+1)} = \frac{\alpha_{n3} + \alpha_{(n+1)4} - \gamma_n}{2}.$$

Thus, the sum of corresponding angles of all "excess flap" surrounding $q_{n,n+m-1}$ is:

$$\sum_{i=n}^{n+m-2} \theta_{Bi} = \frac{\sum_{i=n}^{n+m-2} \alpha_{i3} + \sum_{i=n+1}^{n+m-1} \alpha_{i4} - \sum_{i=n}^{n+m-2} \gamma_i}{2}.$$

Substitute $\sum_{i=n}^{n+m-2} \gamma_i = (m-2) \cdot 180^\circ + \gamma_{n,n+m-1}$ and $\alpha_{n3} + \alpha_{n4} = \alpha_{n5} + 180^\circ$ into the above

result:

$$\sum_{i=n}^{n+m-2} \theta_{Bi} = \frac{\alpha_{n3} + \alpha_{(n+m-1)4} + \sum_{i=n+1}^{n+m-2} \alpha_{i5} + (m-2) \cdot 180^\circ - ((m-2) \cdot 180^\circ + \gamma_{n,n+m-1})}{2}$$

$$\sum_{i=n}^{n+m-2} \theta_{Bi} = \frac{\alpha_{n3} + \alpha_{(n+m-1)4} + \sum_{i=n+1}^{n+m-2} \alpha_{i5} - \gamma_{n,n+m-1}}{2}$$

This result is consistent with Theorem 4:

$$\sum_{i=n}^{n+m-2} \theta_{Bi} = \frac{\alpha_{n3} + \sum_{i=n+1}^{n+m-2} \alpha_{i5} + \alpha_{(n+m-1)4} - \gamma_{n,n+m-1}}{2}.$$

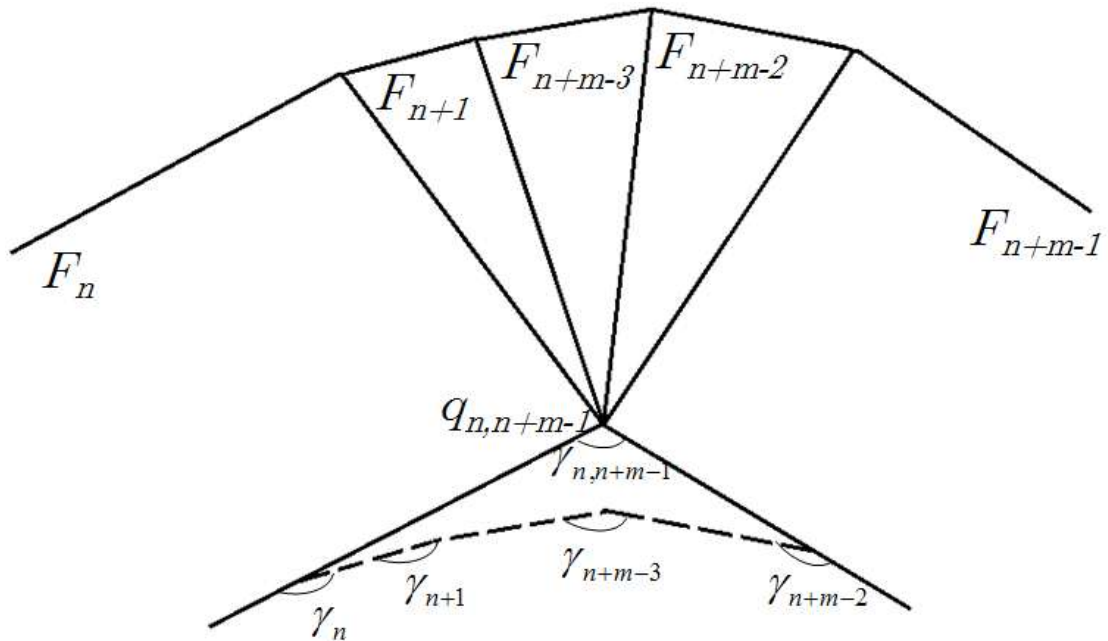


Fig 13: Proof of Corollary 5

4.3 Conditions and Limitations

Proposition 6 Length of middle valley line:

$$d_n = b_n - \frac{t_n (\cos \delta_n + 1) \sin(\alpha_{n3} - \theta_{Bn} + \alpha_{n4} - \theta_{B(n-1)})}{2 \sin(\alpha_{n3} - \theta_{Bn}) \sin(\alpha_{n4} - \theta_{B(n-1)})}.$$

Proof: In General Algorithm step 1, we have obtained middle valley line on all lateral faces. Translate middle valley line to the lower edge of lateral face, $d = b - y - z$. Segments y and z are shown in Fig.14.

By applying trigonometry identity to right-angled triangles with catheti y and x_2 , catheti z and x_2 :

$$y_n = \frac{x_{n2}}{\tan(\alpha_{n4} - \theta_{B(n-1)})} \text{ and}$$

$$z_n = \frac{x_{n2}}{\tan(\alpha_{n3} - \theta_{Bn})}.$$

Substitute $x_2 = \frac{t(\cos \delta + 1)}{2}$ (Eq 4.5 from Proposition 2) into y and z ,

$$d_n = b_n - y_n - z_n$$

$$= b_n - \frac{x_{n2}}{\tan(\alpha_{n4} - \theta_{B(n-1)})} - \frac{x_{n2}}{\tan(\alpha_{n3} - \theta_{Bn})}$$

$$= b_n - \frac{t_n(\cos \delta_n + 1)}{2 \tan(\alpha_{n4} - \theta_{B(n-1)})} - \frac{t_n(\cos \delta_n + 1)}{2 \tan(\alpha_{n3} - \theta_{Bn})}$$

$$= b_n - \frac{t_n(\cos \delta_n + 1) \sin(\alpha_{n3} - \theta_{Bn} + \alpha_{n4} - \theta_{B(n-1)})}{2 \sin(\alpha_{n3} - \theta_{Bn}) \sin(\alpha_{n4} - \theta_{B(n-1)})}$$

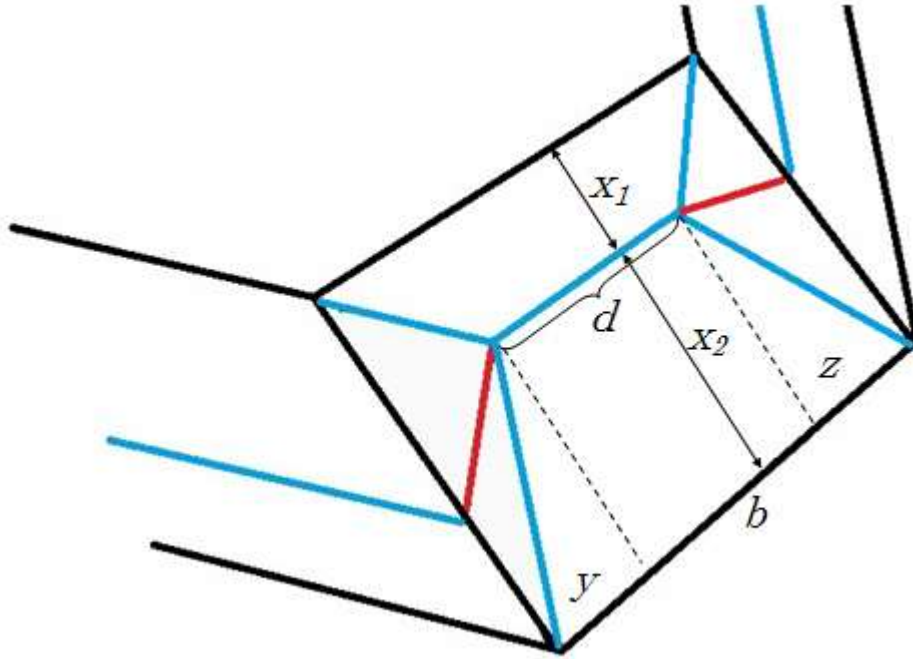


Fig 14: Notations on lateral face

In fact, for each F , there are three possible "five valley line" crease patterns, as shown in Fig. 15.

In the first pattern shown in Fig. 15a, the two end points of middle valley line are intersection point of two valley lines extending from $p_{i,j}$ and $q_{i,j}$ and intersection point of two valley lines extending from $p_{j,k}$ and $q_{j,k}$. Length of middle valley line is positive.

In the second pattern shown in Fig. 15b, four valley lines extending from $p_{i,j}$, $q_{i,j}$, $p_{j,k}$ and $q_{j,k}$ intersect simultaneously. Length of middle valley line is zero.

In the third pattern shown in Fig. 15c, the two valley lines extending from $p_{i,j}$ and $q_{i,j}$ intersect before intersecting with the middle valley line. Length of middle valley line is

negative (shown in dashed line). In this case, limitation exists.

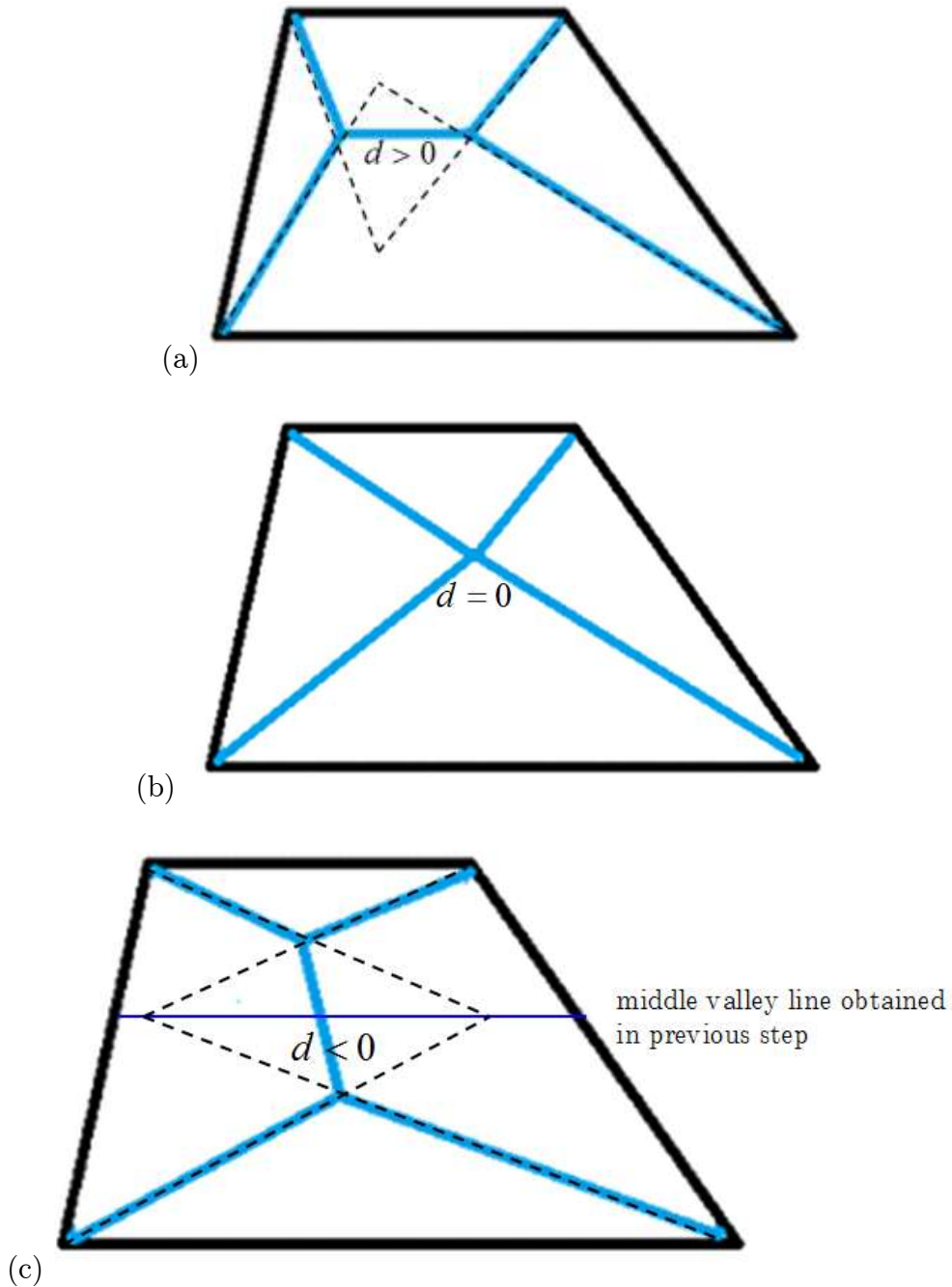


Fig 15: (a) (b) (c) Three possible valley line patterns on quadrilateral lateral face

This problem can be solved using "horizontal slicing". By adding mountain lines parallel to R and B , we "slice" P into two pramatoids P' and $(P-P')$, where P' has the largest possible height without running into limitation (Fig. 16). Upon slicing, roof plane of P' is R' , which is also base plane of $(P-P')$.

Theorem 7 If h' represents height of P' , then

$$h' = h \cdot \max \left(\frac{b_n \cdot 2 \sin(\alpha_{n3} - \theta_{Bn}) \sin(\alpha_{n4} - \theta_{B(n-1)})}{(\cos \delta_n + 1) \sin(\alpha_{n3} - \theta_{Bn} + \alpha_{n4} - \theta_{B(n-1)})} \right) \frac{1}{t_n}$$

Proof: For each F'_n of P' , $d'_n = b_n - \frac{t'_n (\cos \delta_n + 1) \sin(\alpha_{n3} - \theta_{Bn} + \alpha_{n4} - \theta_{B(n-1)})}{2 \sin(\alpha_{n3} - \theta_{Bn}) \sin(\alpha_{n4} - \theta_{B(n-1)})} \geq 0$.

To obtain largest possible height h' , $t'_n = b_n \cdot \frac{2 \sin(\alpha_{n3} - \theta_{Bn}) \sin(\alpha_{n4} - \theta_{B(n-1)})}{(\cos \delta_n + 1) \sin(\alpha_{n3} - \theta_{Bn} + \alpha_{n4} - \theta_{B(n-1)})}$.

Thus, $\frac{h'}{h} = \max \left(\frac{t'_n}{t_n} \right) = \max \left(\frac{b_n \cdot 2 \sin(\alpha_{n3} - \theta_{Bn}) \sin(\alpha_{n4} - \theta_{B(n-1)})}{(\cos \delta_n + 1) \sin(\alpha_{n3} - \theta_{Bn} + \alpha_{n4} - \theta_{B(n-1)})} \right) \frac{1}{t_n}$.

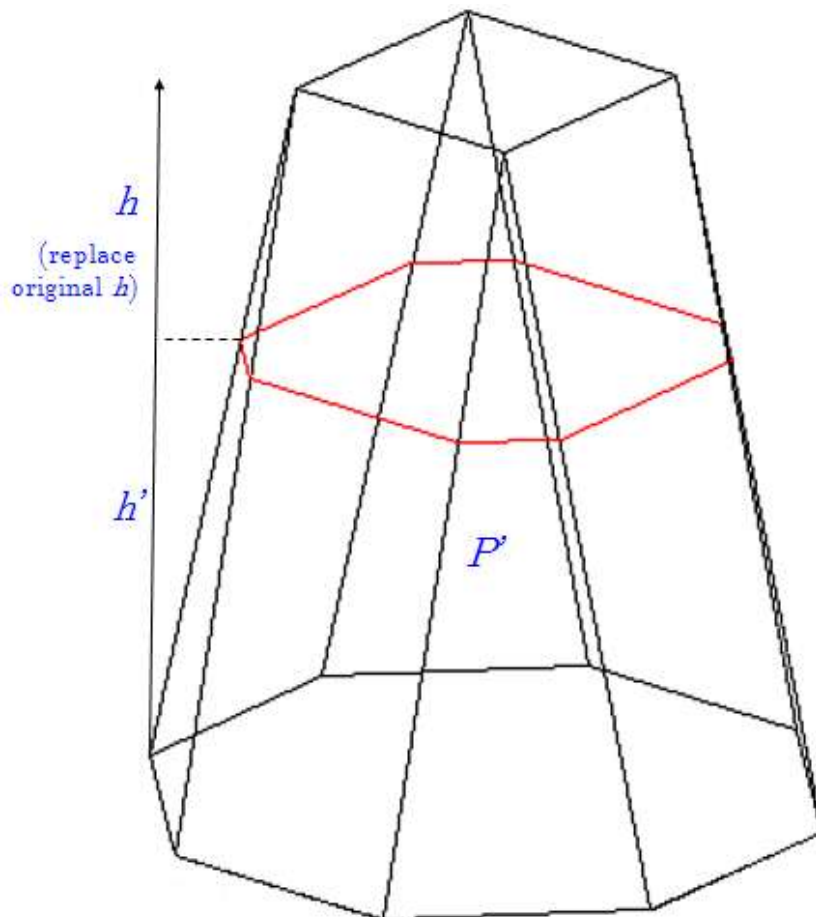


Fig 16: Horizontal slicing

Below shows a crease pattern of a cupola with limitation (Fig. 17).

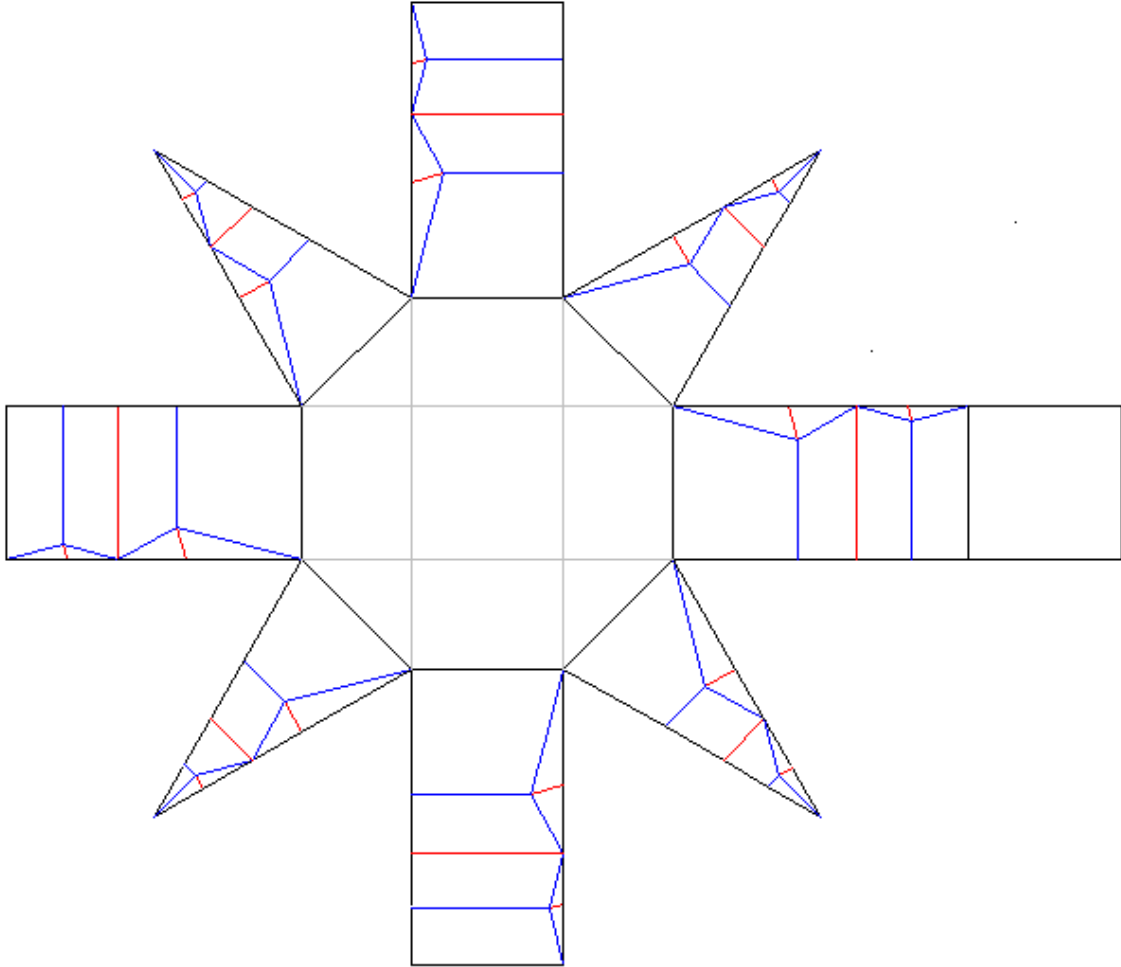


Figure 17: Crease pattern of a cupola with limitation

However, when lateral face F is a triangular lateral face, "horizontal slicing" cannot be applied any longer. The limitation exists when angle of "excess flap" θ_1 overlaps with θ_2 . And $\theta_1 + \theta_2 > \alpha_0$.

Upon "horizontal slicing", θ_1 and θ_2 will remain unchanged, thus cannot solve the limitation.

We propose a rough idea of "sink fold" to solve the limitation on triangular lateral faces.

Since $\theta_1 + \theta_2 \leq \alpha_0$ must be fulfilled, for the ease of calculation, we "sink fold" the excess

part if $\theta > \frac{\alpha_0}{2}$. Below shows an example of a prismaoid where limitations exist on three of the triangular lateral faces (Fig. 18).

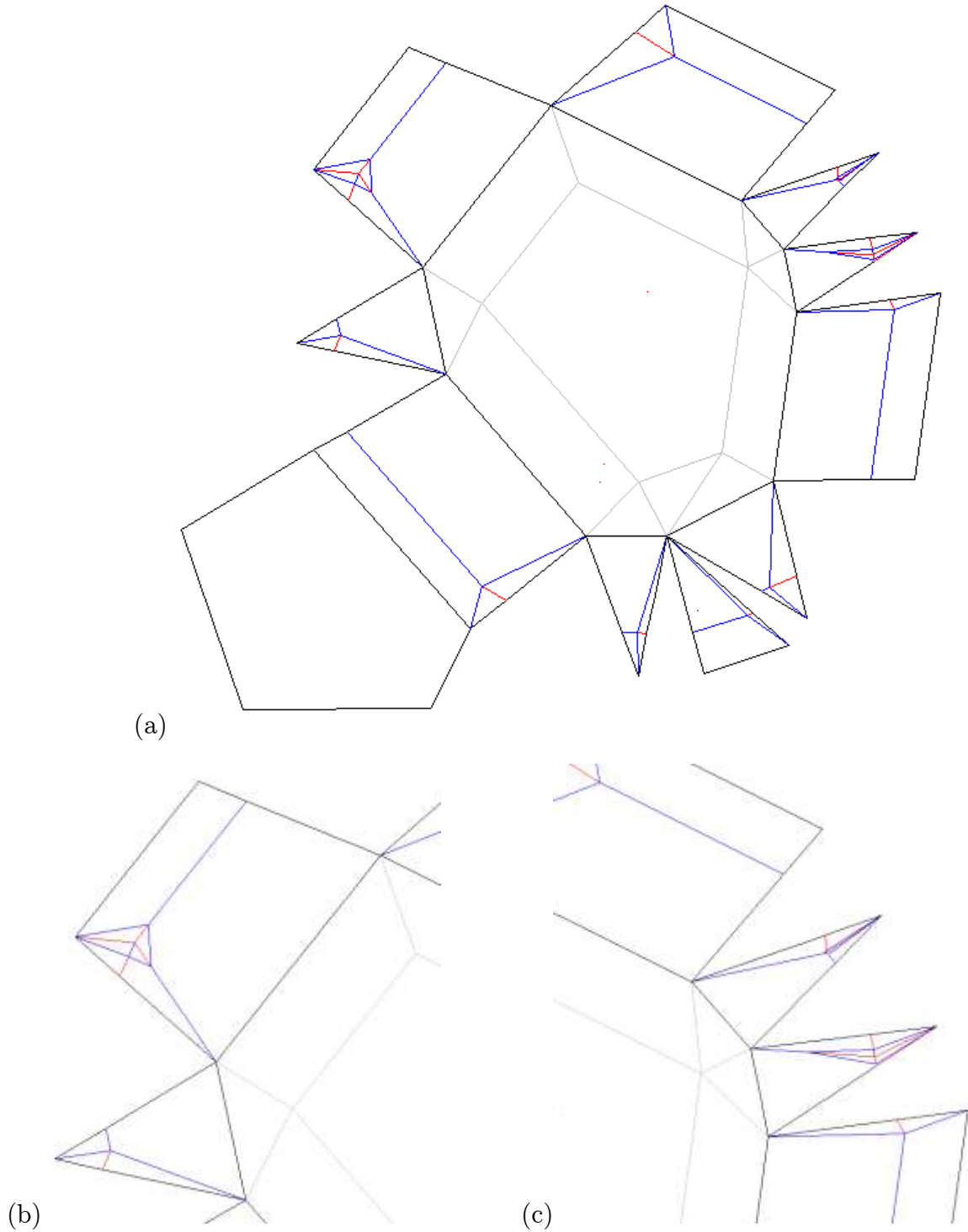


Figure 18: (a) "Sink fold" on triangular lateral faces
 (b) (c) Enlarged details

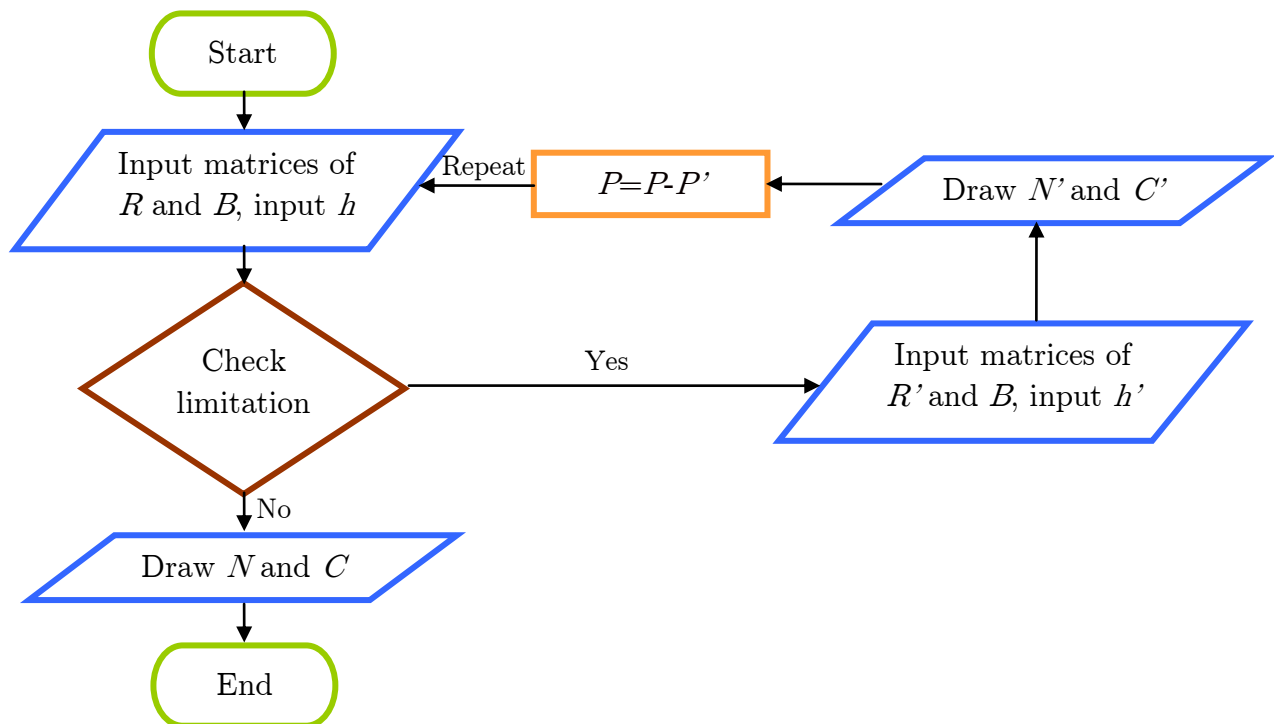
4.4 Mountain lines

Mountain lines appear naturally when we fold along the valley line patterns. When drawing, connect end points of two middle valley lines on every two adjacent lateral faces.

4.5 MATLAB Algorithm

Algorithm Create Pattern of P

- 1: **input** matrices of R and B , input h
 - 2: **if** no limitation
 - 3: Draw N
 - 4: Draw C
 - 5: **else if** limitation exists
 - 6: Calculate h'
 - 7: Input matrices of R' and B
 - 8: Draw N'
 - 9: Draw C'
 - 10: $P=P \cdot P'$
 - 11: repeat from 1
 - 12: **end**
-



5 Implementation and Results

A MATLAB program has been written to implement our proposed algorithm for flattening convex prismaticoids. Users input projection and height of their target prismaticoid. The net and crease pattern are automatically generated by the program and may be printed out to be folded. Examples 1-5 are specifically chosen for their varied structures to illustrate the correctness and capabilities of our proposed algorithm. Projection of each example is drawn. The net and crease pattern for flattening is

obtained by the program. The 3D structure as well as the flattened state of the convex prismaticoid is then shown.

Example 1 (Fig. 19) is a rotationally symmetric frustum. Its layout of roof plane and layout of base plane are similar.

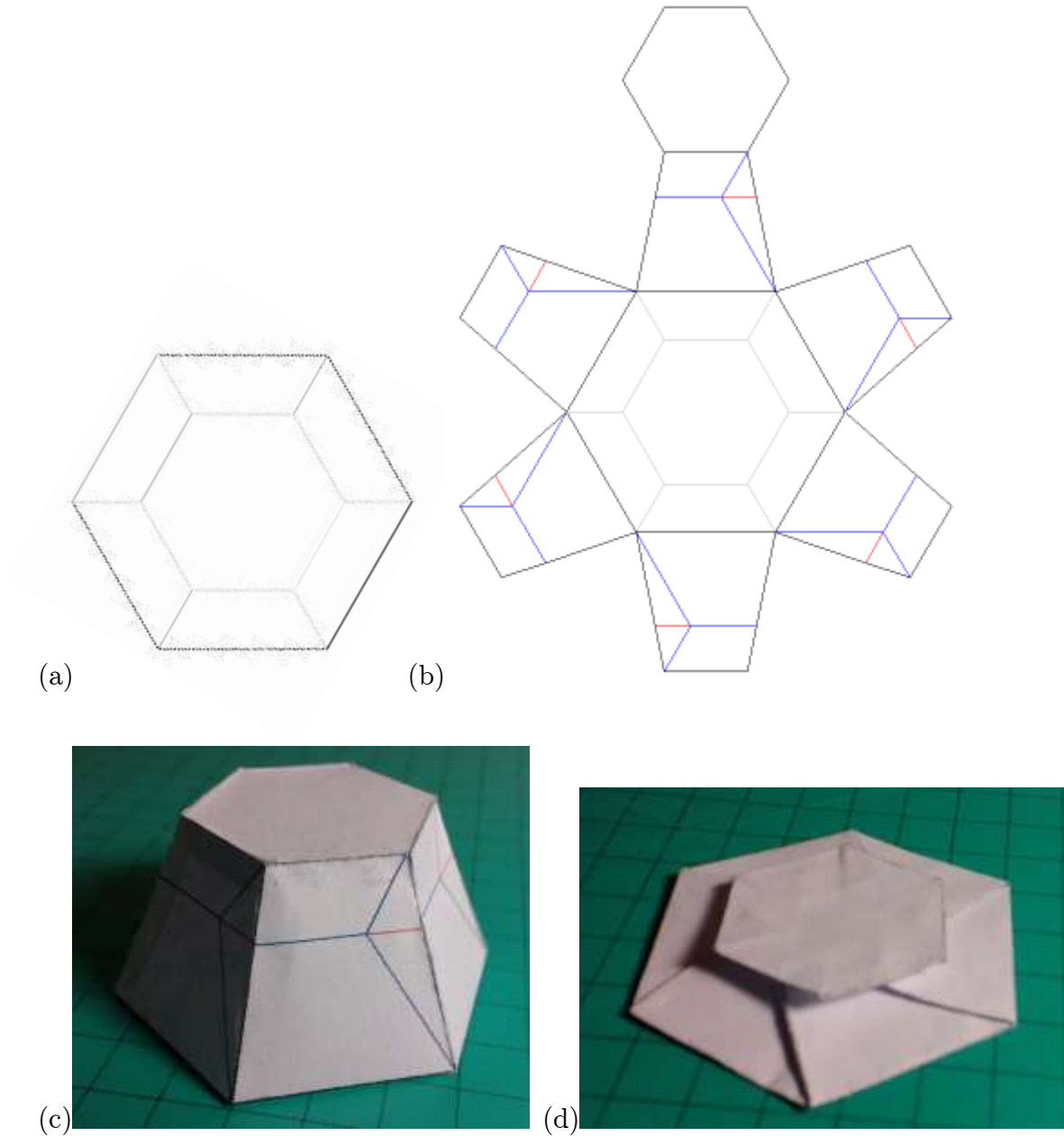


Fig 19: Example 1 (a) The projection (b) The expanded view with crease pattern (b)The convex prismaticoid (d) The flattened product

Example 2 (Fig. 20) is an oblique prism whose roof plane and base plane have the same layout.

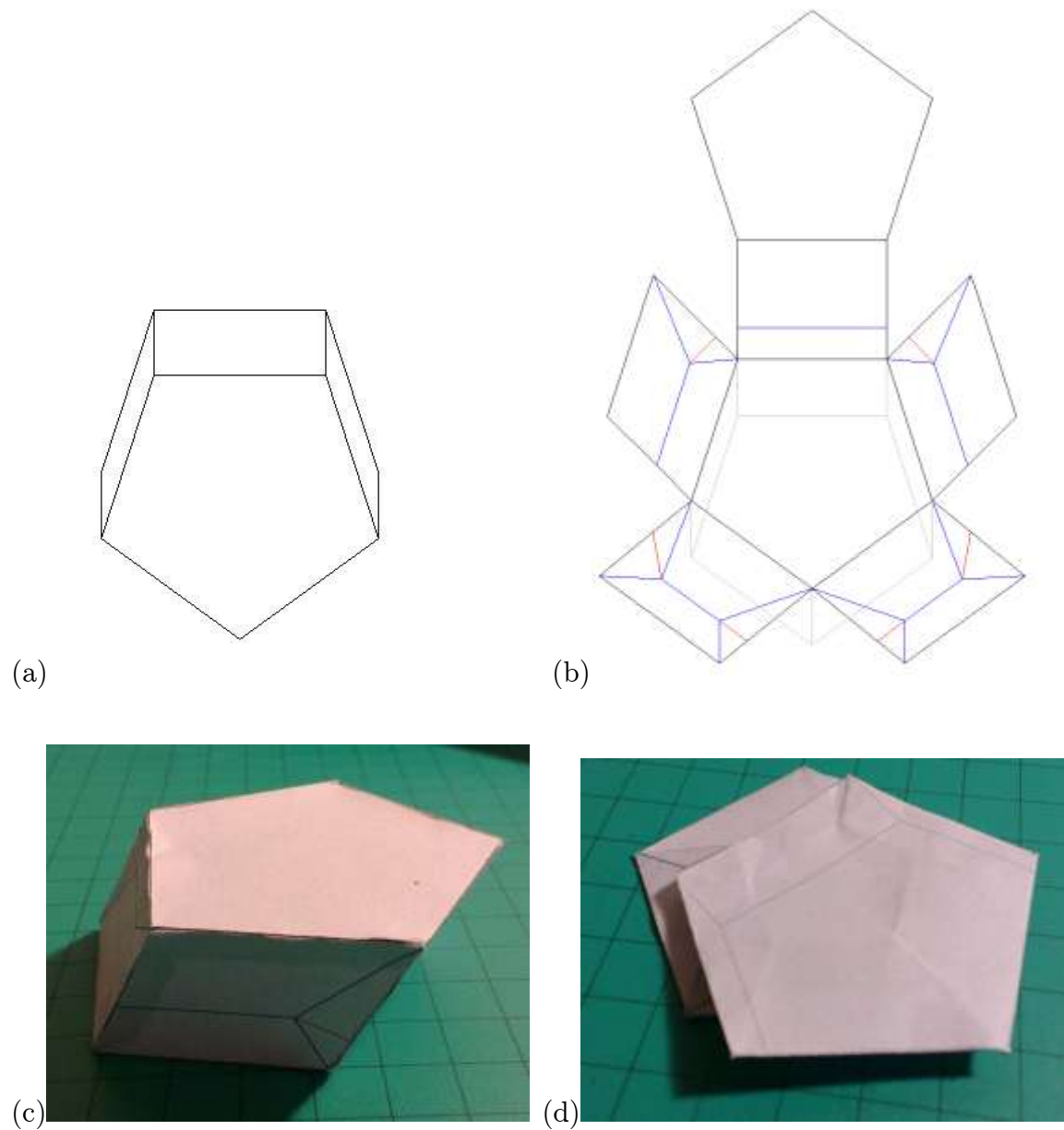


Fig 20: Example 2 (a) The projection (b) The expanded view with crease pattern (c) The convex prismatic (d) The flattened product

Example 3 (Fig. 21) is a cupola, whose base plane has twice vertices as many as its roof plane, and both planes are joined by alternating triangles and rectangles.

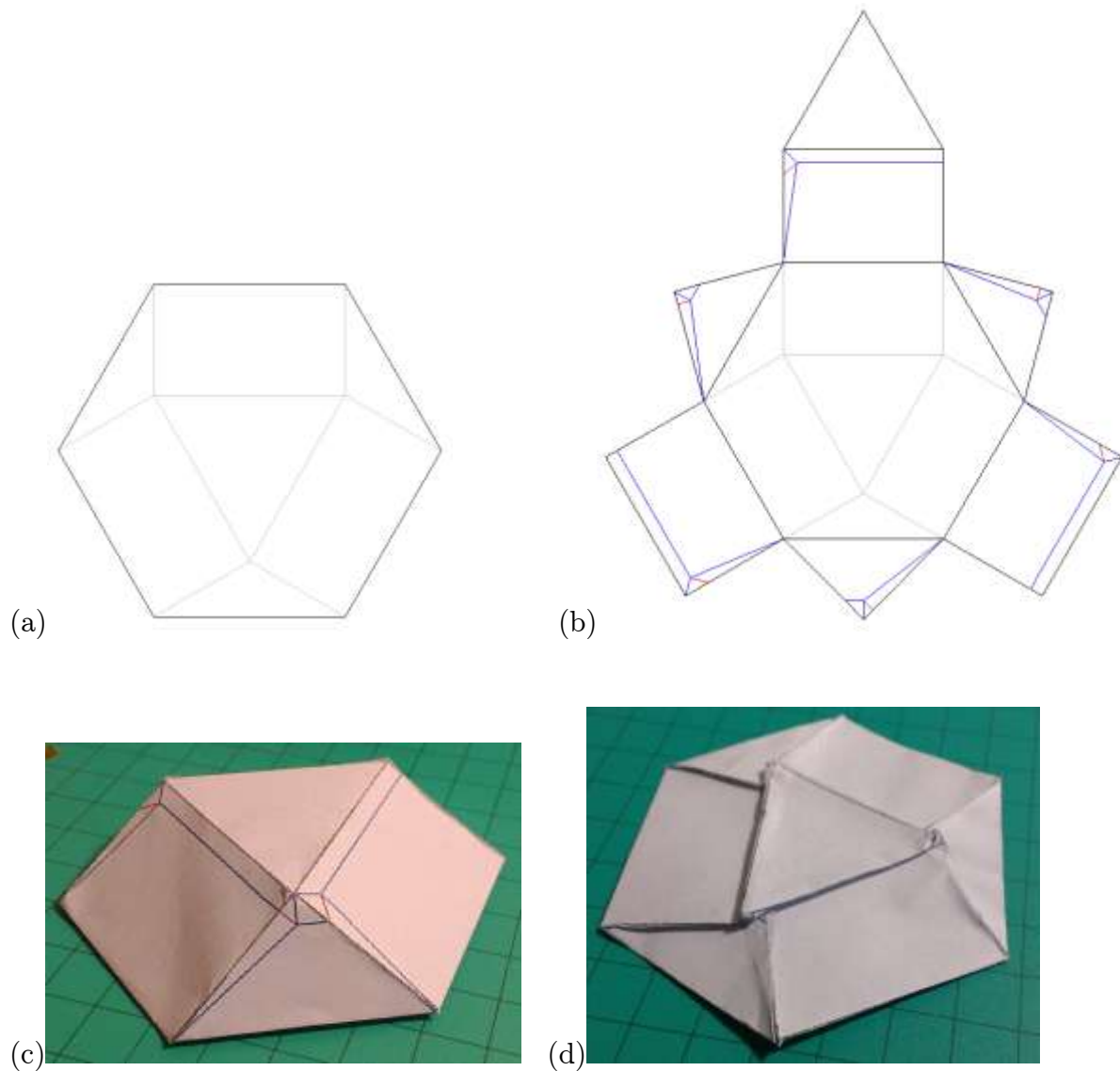


Fig 21: Example 3 (a) The projection (b) The expanded view with crease pattern (c) The convex prismatic (d) The flattened product

Example 4 (Fig. 22) is an antiprism which has only triangular lateral faces.

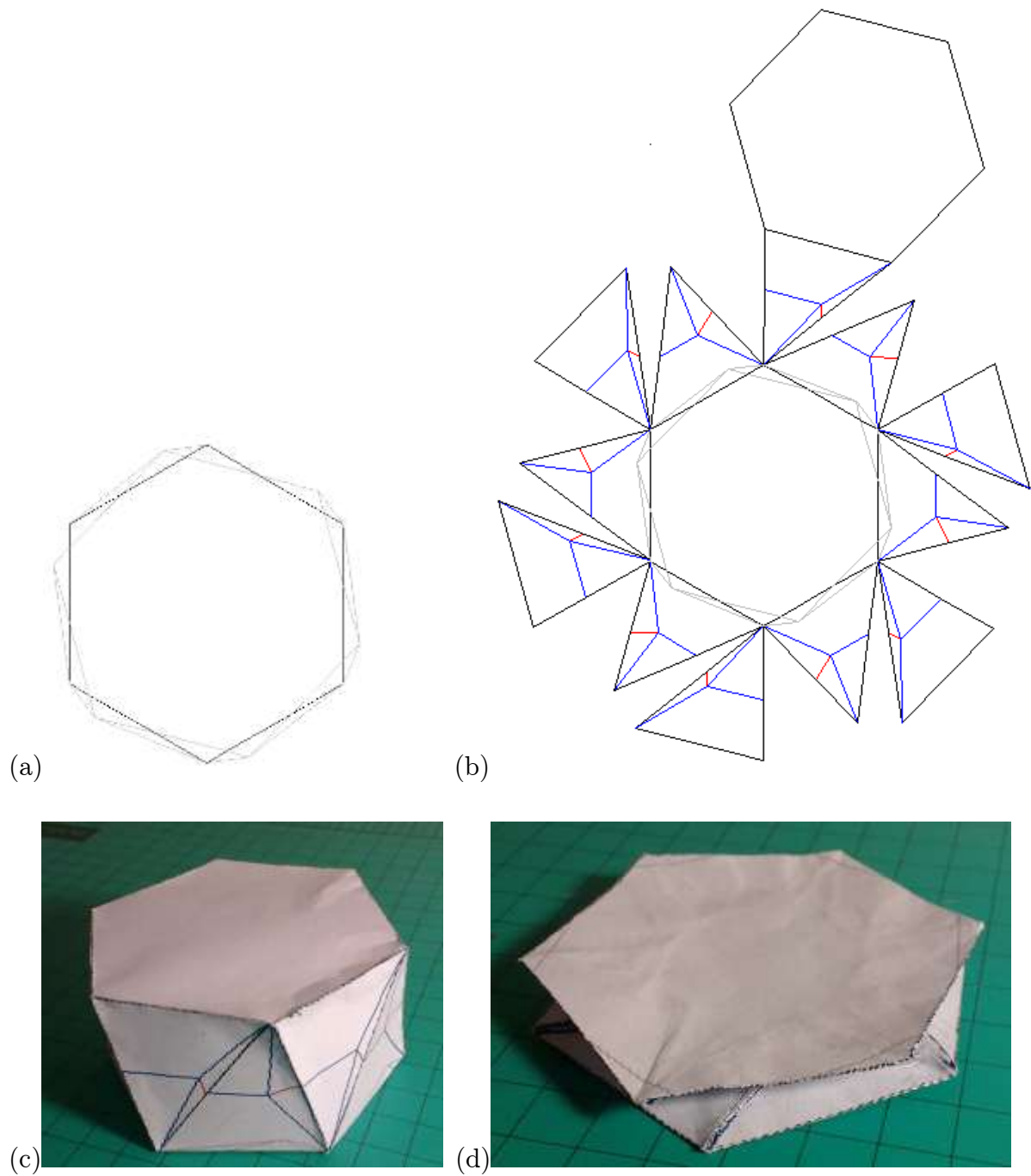


Fig 22: Example 4 (a) The projection (b) The expanded view with crease pattern (c) The convex prismatic (d) The flattened product

Example 5 (Fig. 23) is a convex prismatoid without any limitation.

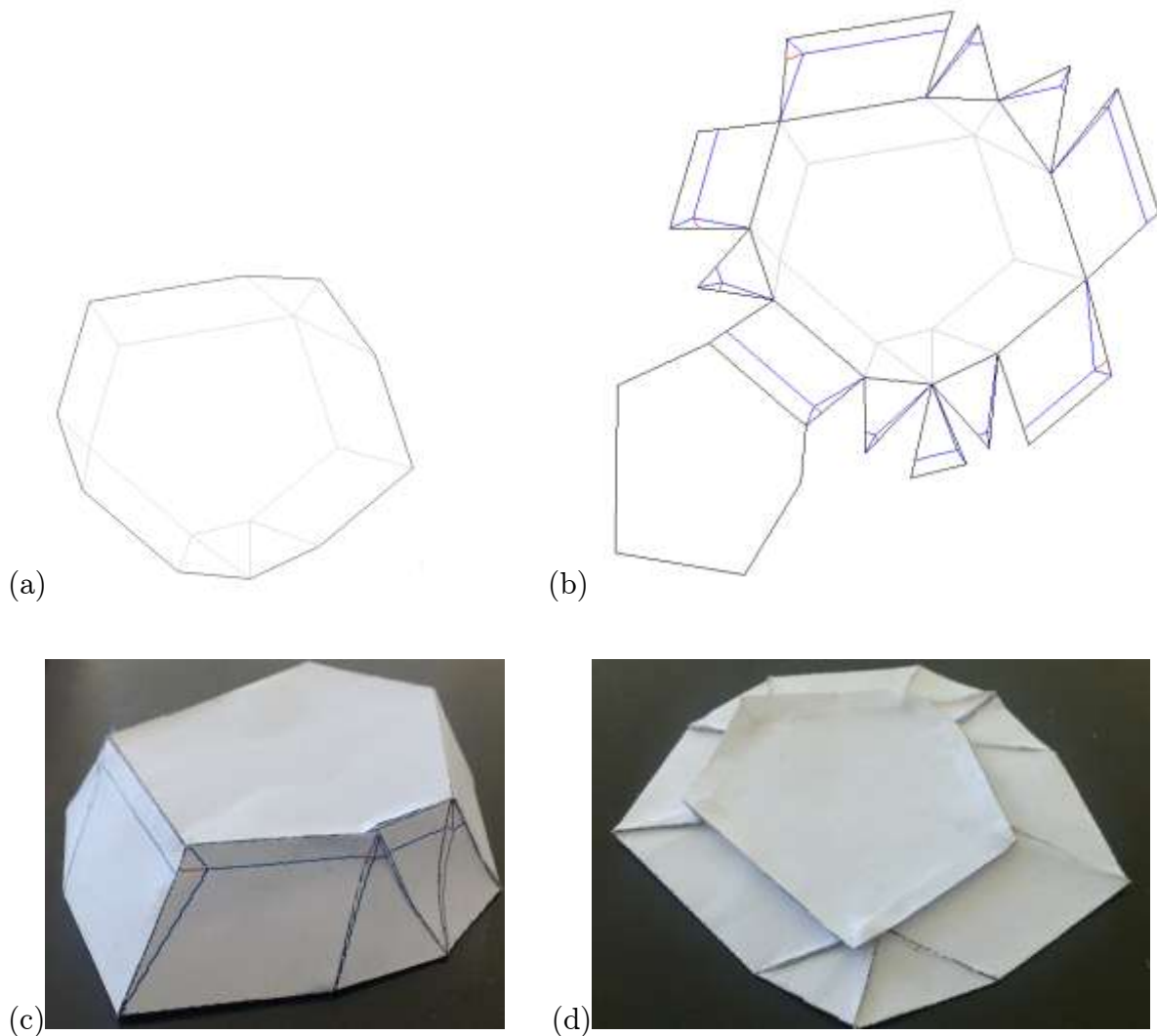


Fig 23: Example 5 (a) The projection (b) The expanded view with crease pattern (c)The convex prismatoid (d) The flattened product

6 Applications

Flattening of polyhedra has many applications in real life. In astronomy, scientists send space telescopes into outer space for observation of distant planets, galaxies, and other outer space objects. If one applies the method of flattening of polyhedron into rigid folding, it may help to reduce the space that the equipment takes up. These equipments can be restored to three-dimensional shape when there is a need to use them [5]. Our work is also applicable to robotics-making. Recently, George M. Whitesides' lab at Harvard has manufactured air-powered origami robotic actuators out of paper and elastic [6]. In the process of restoring the shape of flattened polyhedron, they make use of the force generated by air and lifted a weight which is over 100 times the weight of the actuator itself. Our work is also useful in biomedical appliances. Medical specialists may need trestles to temporarily hold a natural conduit open so that they can complete the

operations successfully. In addition, our method can be applied to stents which are inserted into patients' bodies. The stents are flattened outside and expanded inside the organs to prevent or counteract a localized flow constriction.

7 Conclusion and Future Work

We have derived an original and novel algorithm for flattening convex prisms. This algorithm has been implemented by a MATLAB program that allows users to specify the projection and height of their target prism and generate the crease pattern automatically.

Since any convex polyhedron can be divided into convex prisms by horizontal slicing, there exists possibility of applying our work to flattening all convex polyhedra. In future work, we will also look at convex polyhedra and more complex shapes that are able to be flattened.

References

- [1] Demaine, E.-D.; Demaine, M.-L.: Recent Results in Computational Origami, In Proceedings of the 3rd International Meeting of Origami Science, Math, and Education (OSME 2001), Monterey, California, 2001, 3–16.
- [2] Demaine, E.-D.; O'Rourke, J.: Geometric Folding Algorithms: Linkages, Origami, Polyhedra, Cambridge University Press, New York, 2007.
- [3] Bern, M.; Hayes, B.: Origami Embedding of Piecewise-Linear Two-Manifolds, Lecture Notes in Computer Science, 4957, 2008, 617-629.
- [4] J. Itoh, C. Nara, C. Vîlcu.: Continuous Flattening of Convex Polyhedra, Computational Geometry, 2012, pp85-97.
- [5] Chia, C.-M.-M.; Debnath, S.: Origami and its Applications in Automotive Field, 2nd International Conference, CUTSE, Sarawak, Malaysia, 2009, 46-49.
- [6] S&T News Bulletin, The latest in Science and Technology Research News, 2(7), 2012

**Report on the project “A General Algorithm of Flattening Convex Prismatoids”
by Li Chenglei, Zhou Jingqi (NUS High School)**

In this project, an algorithm for construction of a flattenings of convex prismatoids is developed and implemented in Matlab. This is an interesting problem with a number of potential real world applications.

The committee ranked this project highly because developing such an algorithm requires substantial creativity and mathematical skill. The mathematics involved is elementary, but coming up with ideas which produce a flattening of any prismatoid is far from obvious. Quite complicated geometric considerations are necessary as a background. The committee feels that the merit of the discovery of such an algorithm is comparable to that of proving an interesting mathematical theorem.

The project presentation was very well delivered. It showed that the students' understanding of the material is quite deep. Interesting examples were given, including a demonstration of the Matlab implementation of the algorithm that has been developed.

It has to be said that the project report is not well written. The exposition sometimes is imprecise and some issues remain unclear. Moreover, the English of the report should be improved.

06--YHMA Evaluation Form -- Regional Competition

Instruction: Please fill in all sections. This form is to help the organizers to communicate your assessments and rationales to others in the evaluation process.

Project Title	A general algorithm of flattening convex prisms				
Evaluation level Choose one:	Referee Report	Regional Committee		Regional Presentation	
Selection Criteria (check one in each area below)	Very strong	Strong	Modest	Weak	Not Applicable
Mathematical Contents (1, 4, 5)		X			
Creativity, Originality (2, 3)		X			
Scholarship, Presentation (7)			X		
Demonstrated Teamwork (8)			X		
Impact outside Math (9)			X		
COMMENTS					
Comments related to Criteria 1,4,5	This paper presented a method to flatten convex prisms. The existence of flattening for any polyhedron is proved by Demaine and Hayes. Demaine and O'Rourke presented a method for flattening any polyhedron of disk or sphere topology. However their method requires that the polyhedron to be extended to 4D during the the folding process. In this paper, the authors proposed a method for flattening a special type of convex polyhedron (thus of sphere topology), but avoiding 4D extension. This research belong to the area of polyhedral geometry. All mathematics involved in the paper are elementary. Both the method and the result are correct.				
Comments related to Criteria 2,3	The authors solve an interesting problem using the technique and the method only involving elementary math.				

Overall Recommendation For Presentation	Highly Competitive	Perhaps Competitive	Not Competitive	It is highly competitive	
-----------------------------------------------	-----------------------	------------------------	--------------------	-----------------------------	--